Article

TRANSPARENT PROCESS

THE EMBO JOURNAL

# Polynucleotide kinase–phosphatase enables neurogenesis via multiple DNA repair pathways to maintain genome stability

Mikio Shimada[†], Lavinia C Dumitrache, Helen R Russell & Peter J McKinnon[*]

## Abstract

**Polynucleotide kinase–phosphatase (PNKP) is a DNA repair factor possessing both 5′-kinase and 3′-phosphatase activities to modify ends of a DNA break prior to ligation. Recently, decreased PNKP levels were identified as the cause of severe neuropathology present in the human microcephaly with seizures (MCSZ) syndrome. Utilizing novel murine *Pnkp* alleles that attenuate expression and a T424GfsX48 frame-shift allele identified in MCSZ individuals, we determined how PNKP inactivation impacts neurogenesis. Mice with PNKP inactivation in neural progenitors manifest neurodevelopmental abnormalities and postnatal death. This severe phenotype involved defective base excision repair and non-homologous end-joining, pathways required for repair of both DNA single- and double-strand breaks. Although mice homozygous for the T424GfsX48 allele were lethal embryonically, attenuated PNKP levels (akin to MCSZ) showed general neurodevelopmental defects, including microcephaly, indicating a critical developmental PNKP threshold. Directed postnatal neural inactivation of PNKP affected specific subpopulations including oligodendrocytes, indicating a broad requirement for genome maintenance, both during and after neurogenesis. These data illuminate the basis for selective neural vulnerability in DNA repair deficiency disease.**

**Keywords** DNA repair; neurodevelopment; neurologic disease; polynucleotide kinase–phosphatase

**Subject Categories** DNA Replication, Repair & Recombination; Neuroscience

**DOI** 10.15252/embj.201591363 | Received 23 February 2015 | Revised 19 June 2015 | Accepted 9 July 2015 | Published online 19 August 2015

**The EMBO Journal (2015) 34: 2465–2480**

## Introduction

Normal development and tissue homeostasis strictly depends upon the maintenance of genome integrity. This is key in all tissues, although the nervous system is particularly susceptible to genotoxic stress as revealed by many examples of neuropathology in human inherited DNA repair disorders (McKinnon, 2013; Madabhushi *et al*, 2014). While defects in each of the major DNA repair pathways impact multiple organ systems, disease-causing mutations in the base excision repair/single-strand break repair (BER/SSBR) pathway appear to uniquely affect the nervous system (Caldecott, 2008; McKinnon, 2009, 2013; Iyama & Wilson, 2013).

Base excision repair is critical for repair of frequent DNA damage events such as those arising from oxidative stress and involves multiple components that are assembled by XRCC1, a key scaffold factor in this pathway (Almeida & Sobol, 2007; Caldecott, 2008). Among these, poly(ADP-ribose) polymerase (PARP) is an enzyme that activates signaling by multiple ADP-ribosylation events (Caldecott, 2008; McKinnon, 2013). Other central components include apurinic/apyrimidinic endonuclease 1 (APE1) to initiate the repair of oxidative DNA lesions and polynucleotide kinase–phosphatase (PNKP), an enzyme critical for processing DNA ends prior to DNA ligation (Caldecott, 2008; Iyama & Wilson, 2013). Other end-processing factors such as Aprataxin (APTX) and tyrosyl DNA phosphodiesterase 1 (TDP1) participate in the modification of specific DNA lesions, such as adenylation intermediates or trapped topoisomerase-1 complexes (Ahel *et al*, 2006; Caldecott, 2008).

Among the BER machinery, PNKP, which consists of an N-terminal forkhead-associated (FHA) domain and a C-terminal region that harbors a fused phosphatase and kinase region, hydrolyzes 3′-phosphate groups and promotes phosphorylation of 5′-OH termini (Pheiffer & Zimmerman, 1982; Karimi-Busheri & Weinfeld, 1997; Jilani *et al*, 1999). Of these dual activities, the phosphatase activity appears to be the essential function of PNKP as the efficient repair of DNA lesions resulting from oxidative damage (e.g., DNA ends containing 3′-phosphoglycolate) critically depends upon the 3′-phosphatase function of PNKP (Breslin & Caldecott, 2009), via its interaction with XRCC1. Notably, PNKP has also been shown to associate with XRCC4, a factor involved in the non-homologous end-joining (NHEJ) pathway that repairs DNA double-strand breaks (DSBs), implicating PNKP in both SSBR and DSBR (Chappell *et al*, 2002; Karimi-Busheri *et al*, 2007; Segal-Raz *et al*, 2011; Zolner *et al*, 2011). However, the physiologic role of PNKP and its relevance during either BER or double-strand break repair (DSBR) is unclear.

Despite the essential nature of the BER pathway, there is clearly a difference in tissue requirements for individual components of

Department of Genetics, St Jude Children's Research Hospital, Memphis, TN, USA
*Corresponding author. Tel: +1 901 595 2700; Fax: +1 901 595 6035; E-mail: peter.mckinnon@stjude.org
[†]Current address: Tokyo Institute of Technology, Tokyo, Japan

this pathway. This likely reflects the nature of the damage and/or the threshold for genotoxic stress-induced effects of different cells and tissues (Lee *et al*, 2012a; McKinnon, 2013). Recently, mutations in PNKP were identified as the cause of microcephaly with seizures (MCSZ), a syndrome characterized by profound neurodevelopmental microcephaly but without any obvious extra-neurologic features (Shen *et al*, 2010; Poulton *et al*, 2013; Nakashima *et al*, 2014). Other disease-causing mutations in DNA SSBR factors such as TDP1 or APTX result in pronounced neurodegeneration, but not microcephaly (Date *et al*, 2001; Takashima *et al*, 2002). An understanding of how individual components of this pathway differentially influence tissue homeostasis and how diseases of varied presentation and phenotype arise clearly requires physiologically relevant models. In this study, we have developed a series of unique genetic models for PNKP function that elucidate the requirements of this enzyme during neural development. In doing this, we uncovered important new insights into PNKP function in the nervous system, revealing a preeminent role in maintaining genome integrity during neurogenesis and in postmitotic neurons.

## Results

### PNKP is essential for neurogenesis

To determine the physiologic requirements for PNKP, we generated multiple mutant *Pnkp* alleles to use as a tool to understand how mutation can lead to neurologic disease. We initially generated a conditional *Pnkp* allele by flanking exons 4 through 7 of mouse *Pnkp* with *LoxP* sites to enable cre-mediated gene deletion (Fig 1A). This strategy generates an out-of-frame null allele, predicted to encode a truncated protein producing only an amino terminal peptide lacking any kinase or phosphatase domains. We subsequently generated mice with either embryo-wide or tissue-specific inactivation. We found that inactivation of *Pnkp* in the embryo using Sox2-cre (which drives cre expression in the embryo proper and not in the placenta) resulted in early lethality. Mutant $Pnkp^{Sox2\text{-}cre}$ embryos could not be recovered after embryonic day 9 (E9; not shown). Thus, like germ line deletion of other key components of BER such as XRCC1(Tebbs *et al*, 1999), PNKP is essential for early embryogenesis. In contrast, when *Pnkp* was deleted throughout neural development using *Nestin-cre* (Fig 1B), we found that $Pnkp^{Nes\text{-}cre}$ mice were born at Mendelian ratios, although these mutant mice did not survive past 5 days of age (Fig 1C). Thus, deletion of *Pnkp* even when restricted to the nervous system still resulted in lethality. These data highlight the essential role for PNKP during neural development and contrast the viability of mice after germ line inactivation of other DNA end-processing factors such as APTX or TDP1 (Katyal *et al*, 2007). Even conditional neural deletion of XRCC1, while having a substantial impact on the brain, is viable for many months (Katyal *et al*, 2007; Lee *et al*, 2009).

To establish how PNKP loss impacts neural development, we first analyzed cortical development. The cortex is a laminar structure (Molyneaux *et al*, 2007), and perturbation of neural development often alters the arrangement of these six cortical layers. The $Pnkp^{Nes\text{-}cre}$ cortex showed a marked reduction in size, although the ordered layering of the cortex still occurred (Fig 1D). However, there were reduced numbers of neurons, particularly in later-born upper cortical layers (see Ctip2, Satb2 and Brn2 immunostaining; Fig 1E). We determined whether the reduced number of neurons was a result of cell death or decreased proliferation. During neural development, we observed abundant cell death from E13 onward using TUNEL analysis (Fig 2A). Cell death was widespread throughout the proliferating regions of the developing nervous system and was associated with DNA damage, indicated by increased γH2AX (Fig 2B). A reduction in proliferation was also found as evidenced by a markedly reduced level of BrdU incorporation (Fig 2C), although based on the high level of apoptosis, reduced proliferation is likely a secondary event. Conspicuously, PNKP loss is substantially more severe than inactivation of either LIG4 or XRCC1, indicating that this enzyme may be involved in the repair of a broader range of DNA lesions that either XRCC1 or LIG4 alone (Fig 2). To further assess PNKP function during corticogenesis, we also used *Emx1-cre*, in which gene deletion occurs around 1 day earlier than *Nes-cre*, and progenitors targeted by *Emx1-cre* have a heightened sensitivity to DNA damage at this early stage (Lee *et al*, 2012a). Accordingly, in contrast to *Nes-cre*, the cortices of $Pnkp^{Emx1\text{-}cre}$ mice were dramatically more affected, showing loss of all dorsal telencephalic progenitors via apoptosis, resulting in an almost complete absence of the cortex (Appendix Fig S1).

To ascertain the effector pathway responsible for cell loss, we generated $Pnkp^{Nes\text{-}cre}$ mice that were also deficient for either p53 or ATM (Appendix Fig S2). P53 is an essential effector after DNA DSBs in all immature cells in the nervous system, while ATM is primarily required for DNA damage-induced apoptosis in immature postmitotic neurons, rather than replication-associated damage (Lee *et al*, 2001; Orii *et al*, 2006). We found that apoptosis in $(Pnkp;Atm)^{Nes\text{-}cre}$ was identical to $Pnkp^{Nes\text{-}cre}$, while p53 inactivation abrogated apoptosis (Fig 3A). Consequently, $(Pnkp;p53)^{Nes\text{-}cre}$ mice were born with a substantially more developed cortex compared with $Pnkp^{Nes\text{-}cre}$ mice (Appendix Fig S2). This is also apparent by recovery of neuronal numbers and a more ordered cortical lamination as assessed by Satb2 and Ctip2 localization in $(Pnkp;p53)^{Nes\text{-}cre}$ mice (Fig 3B). Thus, PNKP loss activates a p53-dependent DNA damage-induced apoptotic pathway.

Cerebellar neurons including the granule neurons in the EGL and particularly the interneurons (comprising the stellate, basket and golgi cells) are susceptible to multiple types of DNA damage. For example, interneurons fail to undergo postnatal expansion after XRCC1 loss due to a p53-dependent cell cycle arrest, while inactivation of essential homologous recombination (HR) factors or telomere uncapping results in p53-dependent apoptosis (Lee *et al*, 2009, 2014). We found that PNKP inactivation also resulted in loss of this cerebellar neuronal population in an ATM-independent, but (partially) p53-dependent manner, with an approximately 40% recovery of interneurons (Fig 3C). Interneuron loss involved elevated γH2AX and apoptosis, indicated by increased TUNEL-positive cells in the cerebellar white matter (Fig 3A). The partial interneuron rescue in the $(Pnkp;p53)^{Nes\text{-}cre}$ cerebellum compared to XRCC1 inactivation, where associated p53 loss resulted in full interneuron recovery, likely reflects the requirement of PNKP for the repair of a broader range of DNA lesions (Lee *et al*, 2009, 2014) (Fig 1, and see below).

 

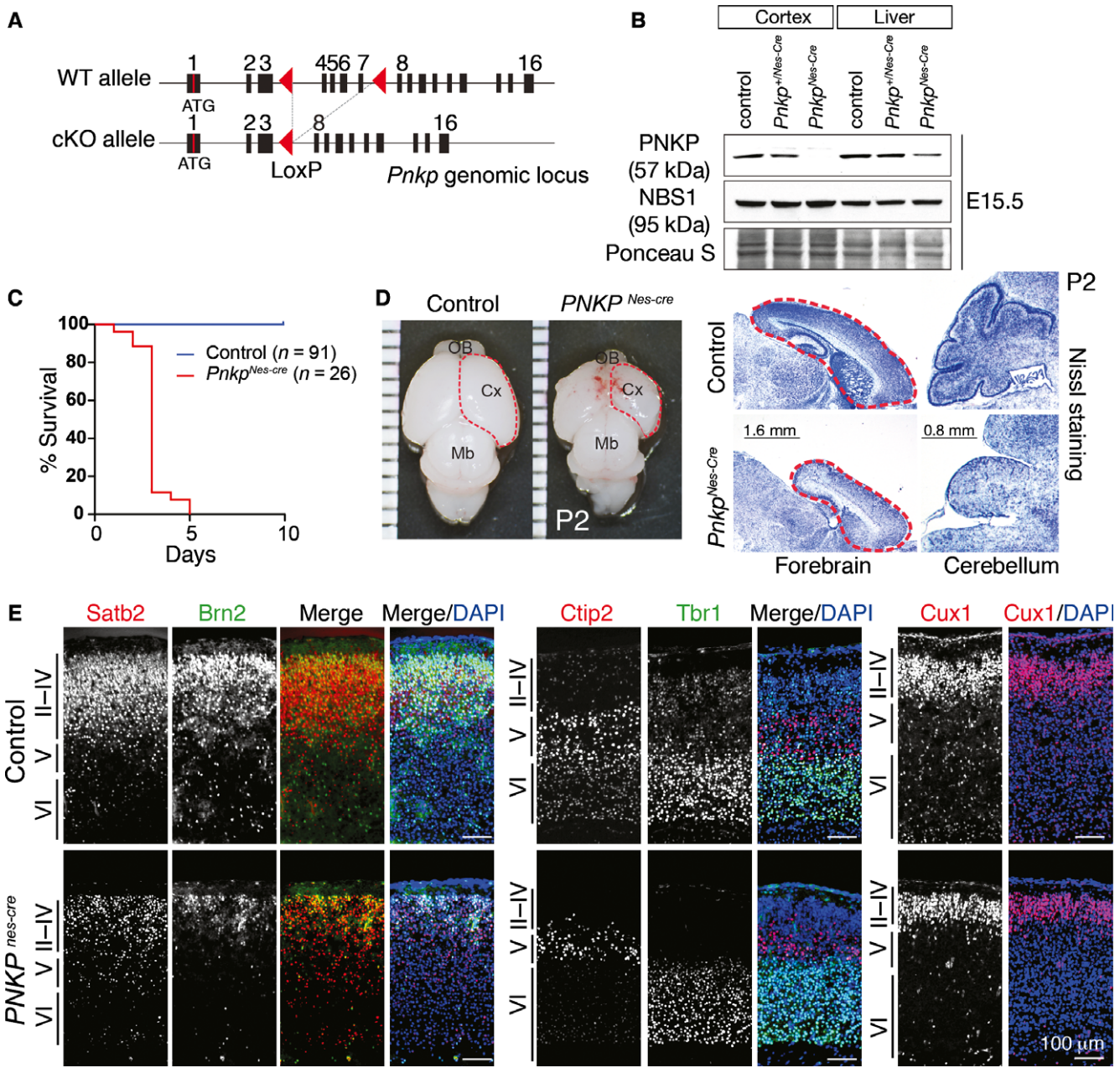


**Figure 1. PNKP is essential factor in neurogenesis.**

A A conditional *Pnkp* allele (cKO) was generated by flanking exons 4 through 7 with *LoxP* sites. Cre-mediated excision generated a transcript that joined exons 3 and 8, thereby changing the *Pnkp* reading frame to a premature stop codon leading to a truncated protein.

B Western blot analysis showed that $Pnkp^{Nes\text{-}cre}$ mice underwent inactivation of PNKP in neural tissues (the cortex) but not tissues outside of the nervous system (the liver). NBS1 is used as an internal standard, and Ponceau staining indicates equivalent protein transfer.

C $Pnkp^{Nes\text{-}cre}$ mice were born alive, but failed to survive past 5 days of age.

D Loss of PNKP markedly affected development of the brain as reduction in the size of the cortex (red-hatched lines) and cerebellum is observed in brain photographs and Nissl-stained sagittal sections.

E While PNKP loss affected brain development by a reduction in overall cell number, the ordered six-layer lamination present in the cortex is nonetheless still maintained in the mutant (indicated by roman numerals).

### PNKP is critical for both BER and NHEJ

Polynucleotide kinase–phosphatase is a dual-function kinase/phosphatase, which processes damaged DNA ends to enable ligation (Weinfeld *et al*, 2011). In particular, the 3′-phosphatase activity is the critical functionality for SSBR after oxidative DNA damage (Breslin & Caldecott, 2009; Weinfeld *et al*, 2011). Polynucleotide kinase–phosphatase has also been linked to the repair of DSB

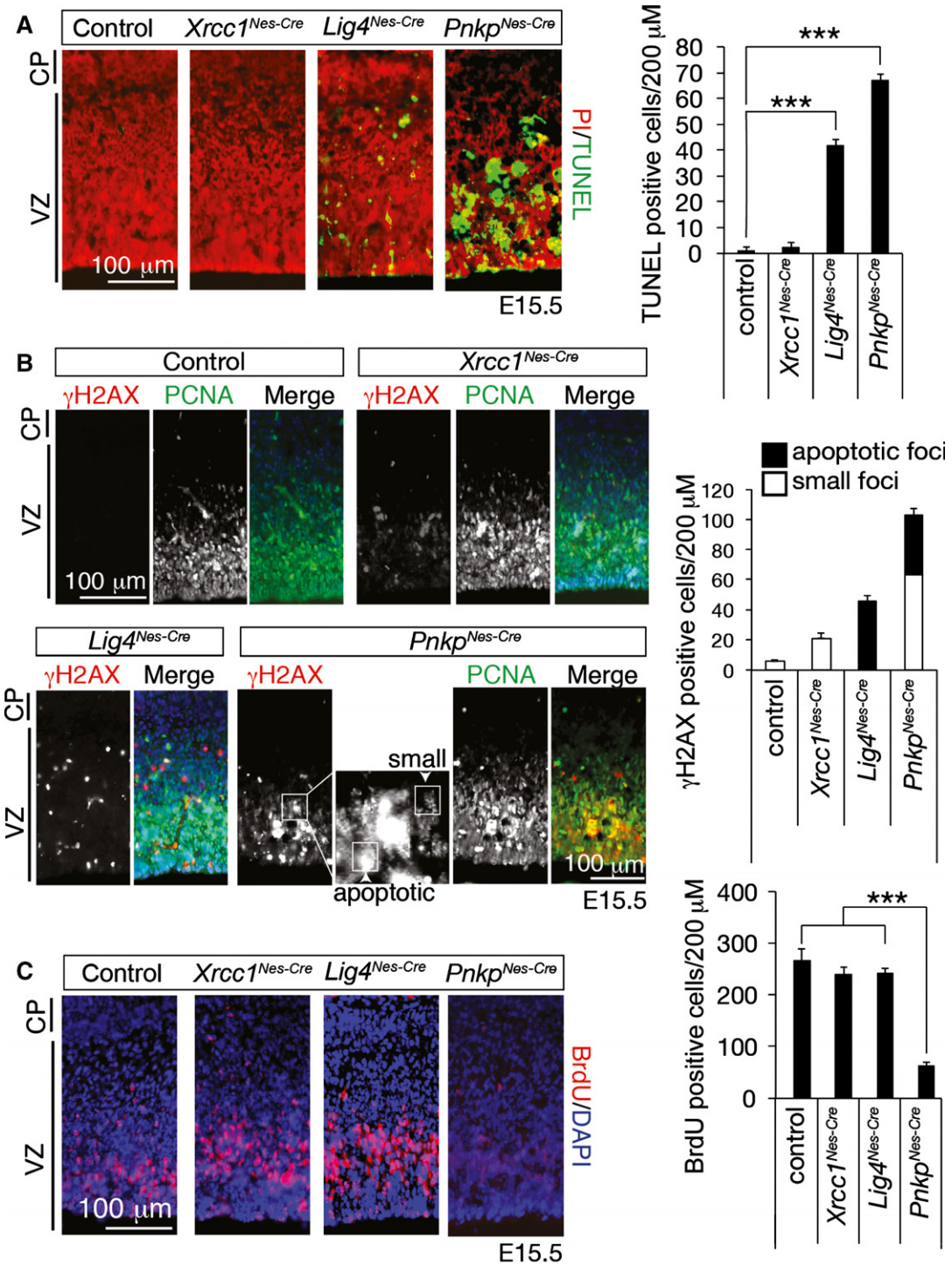


**Figure 2. PNKP prevents DNA damage-induced apoptosis in the developing nervous system.**

A TUNEL (green) with propidium iodide (PI, red) counterstaining identifies abundant apoptosis in the E15.5 developing nervous system of the *Pnkp*$^{Nes\text{-}cre}$ embryo compared to the base excision repair mutant *Xrcc1*$^{Nes\text{-}cre}$ and the NHEJ mutant *Lig4*$^{Nes\text{-}cre}$ or wild-type controls. TUNEL-positive cells are quantified in the graphs opposite. ***$P < 0.0003$.

B Loss of PNKP resulted in DNA damage as indicated by γH2AX immunostaining, both as small nuclear puncta indicating DNA damage and also as large diffuse apoptotic foci. *Xrcc1*$^{Nes\text{-}cre}$ and *Lig4*$^{Nes\text{-}cre}$ are shown as a comparison to *Pnkp*$^{Nes\text{-}cre}$. Quantitative data are shown on adjacent graphs. PCNA immunostaining was used to identify proliferating cells.

C BrdU incorporation shows there is a marked reduction in cell proliferation in the *Pnkp*$^{Nes\text{-}cre}$ embryonic tissue compared to either *Xrcc1*$^{Nes\text{-}cre}$ or *Lig4*$^{Nes\text{-}cre}$. Adjacent graphs are quantitative representation of the immunostains. ***$P < 0.005$.

Data information: For (A–C) the mean (± SD) results from at least 3 replicates.

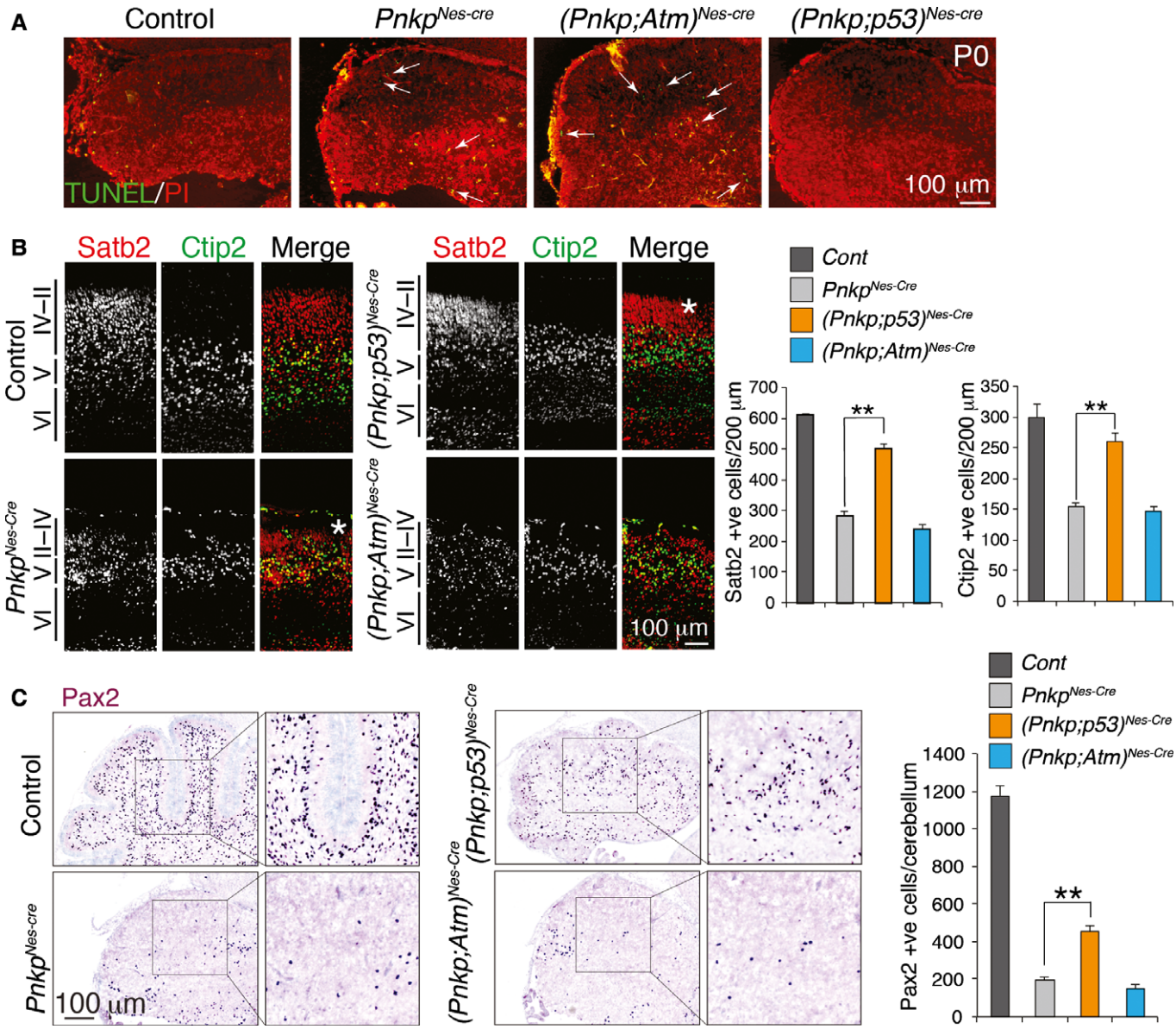


**Figure 3. PNKP loss targets multiple cell types and involves p53 signaling.**

A PNKP loss results in apoptosis in the developing cerebellum as shown using TUNEL (green) with propidium iodide (PI, red) counterstaining. Apoptosis is substantially rescued by p53 inactivation but not ATM inactivation. Arrows indicate apoptotic cells.

B Cell loss after inactivation of PNKP involves p53, but not ATM, as illustrated by rescue of upper layer neurons in $(Pnkp;p53)^{Nes\text{-}cre}$ tissue (identified by Satb2 immunostaining); asterisks indicate relative cortical rescue of $Pnkp^{Nes\text{-}cre}$ after p53 loss. Graphs quantify rescue after p53 loss. The mean (± SD) results from 3 independent sections. $^{**}P < 0.006$.

C Cerebellar interneurons (identified by Pax2 immunostaining) are also susceptible to PNKP loss and occur in a partially p53 manner. Data is the mean value of triplicate sections, error bars represent ± SD. $^{***}P < 0.001$.

lesions (Chappell *et al*, 2002; Karimi-Busheri *et al*, 2007; Segal-Raz *et al*, 2011; Zolner *et al*, 2011), although the direct importance of PNKP in DSBR is less firmly established than for BER. We reasoned that the increased impact of PNKP loss on neurogenesis (e.g., compared to XRCC1) reflects deficits in both BER and DSBR. To determine the importance of PNKP for repair of different DNA lesions, we established $Pnkp^{Nes\text{-}cre}$ primary cortical astrocytes and those derived from other mutant mice defective in BER or NHEJ. Using the comet assay, we found a significant deficiency in the repair of DNA damage in $Pnkp^{Nes\text{-}cre}$ cells after treatment with ionizing radiation (IR), hydrogen peroxide ($H_2O_2$) or camptothecin (CPT) in non-replicating astrocytes, as shown by increased DNA strand breaks after recovery from genotoxin treatment (Fig 4A). Thus, loss of PNKP compromises DNA repair after a variety of genotoxins.

Because these cells were non-replicating, $H_2O_2$ and CPT produce DNA SSBs, while IR produces both SSBs and DSBs. To establish whether the DNA repair deficiency in the PNKP-null cells also

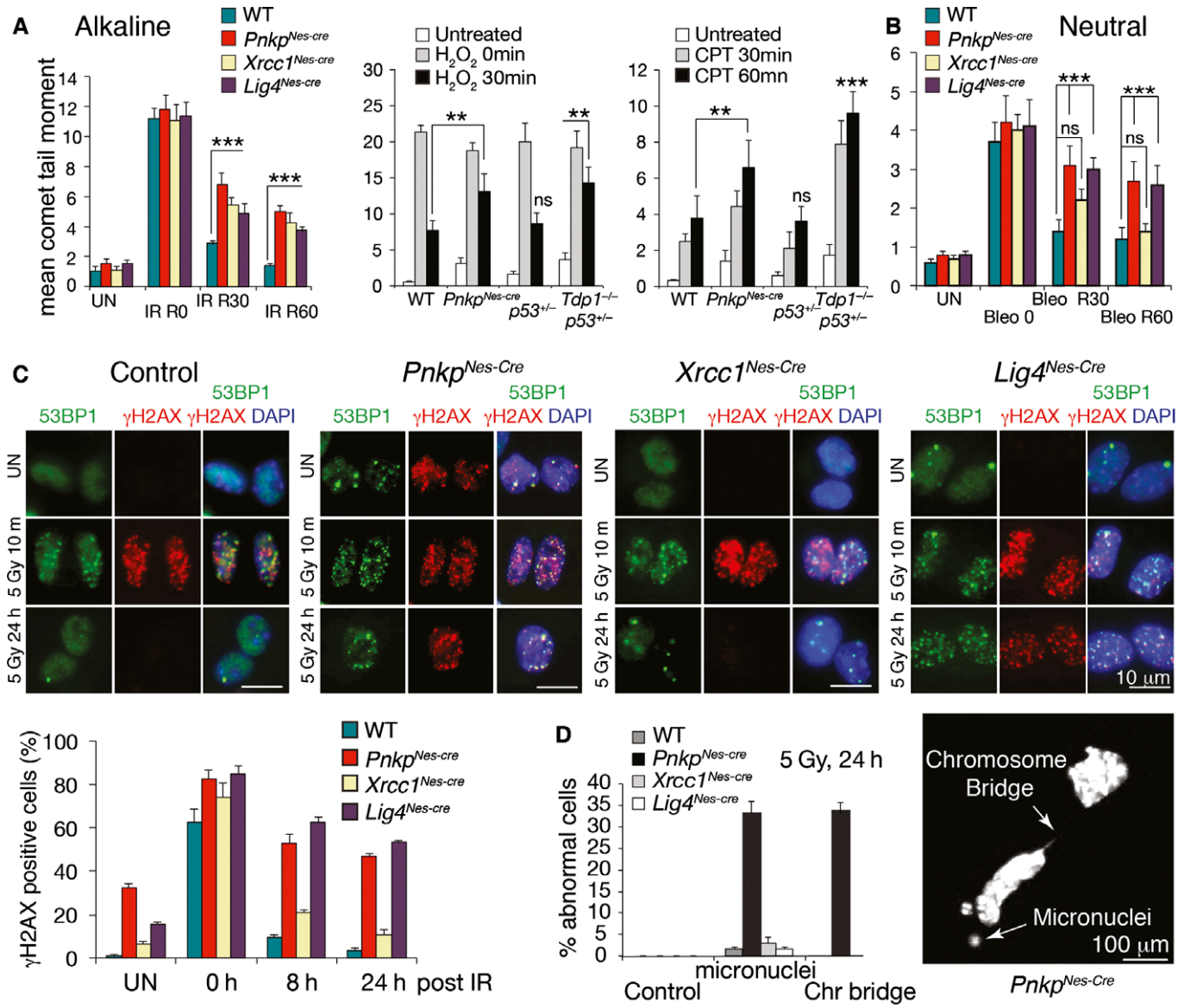


**Figure 4. PNKP is essential for DNA repair by both base excision repair and non-homologous end-joining.**

A Genotoxins that cause single- (IR, $H_2O_2$ and CPT) and double (IR)-strand breaks in non-replicating (density arrested) primary astrocytes show a repair deficiency after PNKP loss via the alkaline comet assay. IR is ionizing radiation, $H_2O_2$ is hydrogen peroxide and is used at 4°C to restrict DNA damage to single-strand breaks, and CPT is camptothecin. ***$P < 0.0001$, **$P < 0.06$.

B Primary *Pnkp*$^{Nes\text{-}cre}$ astrocytes show a defect in the repair of DNA DSBs after bleomycin treatment when analyzed using the neutral comet assay system. The alkaline comet assay identifies both SSBs and DSBs while the neutral comet assay identifies DSBs. ***$P < 0.0001$; ns, not significant.

C Recovery of the DSB markers, γH2AX and 53BP1, are defective in *Pnkp*$^{Nes\text{-}cre}$ astrocytes after IR as it is in the *Lig4*$^{Nes\text{-}cre}$ NHEJ mutant, while the *Xrcc1*$^{Nes\text{-}cre}$ base excision repair mutant is not defective in NHEJ. Quantitation of γH2AX removal is presented graphically.

D *Pnkp*$^{Nes\text{-}cre}$ primary astrocytes also show frequent micronuclei formation after radiation, in a manner distinct to *Lig4*$^{Nes\text{-}cre}$ or *Xrcc1*$^{Nes\text{-}cre}$. Chromosome bridges are also found in *Pnkp*$^{Nes\text{-}cre}$ astrocytes after radiation as shown in the photomicrograph.

Data information: For (A–D) the mean (± SD) results from at least 3 experimental replicates.

involved defective DSBR, we used a neutral comet assay. In this experiment, we used bleomycin, an agent that generates a higher relative frequency of DNA DSBs to SSBs. We found that inactivation of PNKP reduces DSBR to levels similar to those after inactivation of the NHEJ factor, Lig4 (Fig 4B). In contrast, disabling the BER pathway via loss of XRCC1 did not impact repair of DSBs. Thus, PNKP is important for repair of DNA DSBs. We further determined whether PNKP loss involved defective NHEJ by inhibiting DNA-PKcs in control and *Pnkp*$^{Nes\text{-}cre}$ cells (Appendix Fig S3). DNA repair was reduced after inhibition of DNA-PKcs using NU7026 in WT primary astrocytes (a repair defect comparable to *DNA-PKcs*$^{-/-}$ astrocytes), while similar treatment of PNKP-deficient cells showed no additional reduction in DNA repair capacity (Appendix Fig S3), suggesting the loss of PNKP was epistatic to defective NHEJ.

 

This finding was reinforced by γH2AX recovery assays to monitor DSBR, and showed that $Pnkp^{Nes\text{-}cre}$ cells had a similar defect in DNA repair to LIG4 loss when compared to controls or those with XRCC1 inactivation (Fig 4C). We also observed widespread chromosomal lesions after IR as indicated by micronuclei and chromosome bridges in a high percentage of PNKP-null cells compared to those with either BER or NHEJ deficiency (Fig 4D). Collectively, these data indicate that loss of PNKP impacts both BER and NHEJ.

#### PNKP is not required for homologous recombination

Given the DNA DSBR deficiency of PNKP-null cells, we also determined whether PNKP was required for DSBR via HR. To do this, we exposed PNKP-null cells to either mitomycin C (MMC) or cisplatin, both of which promote interstrand crosslinks, which requires HR for repair (Deans & West, 2011). We assessed RAD51 foci removal after DNA breaks as a measure of HR and included HR-defective BRCA2-null primary astrocytes as a control. We found that after MMC or cisplatin treatment, PNKP-null cells were similar to controls in removal of RAD51 damage-induced foci (Fig 5A; although basal γH2AX is higher in PNKP-null cells). In contrast, BRCA2 null cells failed to assemble RAD51 foci and were also deficient in γH2AX resolution (Fig 5). Primary $Atm^{-/-}$ astrocytes were also included as an additional control as they had been reported to be defective in HR (Morrison *et al*, 2000), although recent data (Kass *et al*, 2013; Rass *et al*, 2013), and our current data (Fig 5), show that they are not HR deficient. A similar dispensability for PNKP during HR was also reported in glioma cells via analysis of sister chromatid exchange (Karimi-Busheri *et al*, 2007). Thus, our findings indicate that PNKP is critical for chromosomal DNA repair via both BER and NHEJ, but not by HR.

#### The *Pnkp* MCSZ allele is lethal in the mouse germ line

The above data indicate that PNKP is an essential DNA repair factor utilized by different DNA repair pathways and that its loss impacts cellular genome stability in the face of endogenous DNA damage. Furthermore, the phenotype of the $Pnkp^{Nes\text{-}cre}$ mouse highlights this enzyme as a key determinant for genome stability that is required for neural development. MCSZ results from hypomorphic mutation in *PNKP* and is notable as the symptomatic pathology is consistent with PNKP being involved in repair of DNA SSBs rather than DSBs (Shen *et al*, 2010; McKinnon, 2013; Poulton *et al*, 2013).

While the PNKP mutations in MCSZ target the kinase region, these mutations also lead to reduced levels of PNKP protein and overall enzyme activity, affecting 3′-phosphatase activity (Shen *et al*, 2010; Reynolds *et al*, 2012). Therefore, we sought to determine how disruption of PNKP produces the characteristic neuropathology in MCSZ by generating a murine T424GfsX48 allele found in multiple MCSZ families (Shen *et al*, 2010; Poulton *et al*, 2013; Nakashima *et al*, 2014). This mutation generates a frame-shift allele of *PNKP* resulting in the insertion of an additional 48 aa at residue 385 and a premature stop codon and truncated protein. Although we were able to identify the expected *Pnkp* mutant message in $Pnkp^{+/T424GfsX48}$ heterozygous mice (levels of MCSZ transcript were reduced to around 20% of the WT allele), we could not recover any E9 (or later) homozygous $Pnkp^{T424GfsX48}$ mutant mice. We were also unable to rescue the lethality of homozygous mutant mice with concomitant loss of p53 or to recover homozygous mutants after outbreeding multiple generations to the highly robust NIMR mouse strain. Unlike humans, the early lethality of the MCSZ embryos suggests that the impact of reduced PNKP levels more substantially impacts early development in the mouse. Unfortunately, this early lethality precluded analysis of MCSZ mutation in the mouse nervous system. Thus, we conclude that reduced PNKP levels become critical in murine tissue, while the low PNKP levels found in humans support viability.

#### Reduced *Pnkp* expression causes neurodevelopmental defects

To generate a scenario mirroring the MCSZ syndrome in the mouse, we utilized an intermediate created during construction of the conditional *Pnkp* allele in which a *Neo* selection cassette was inserted into intron 4 (Fig 6A; this allele is termed $Pnkp^{Neo}$). Analysis of tissues from the $Pnkp^{Neo/Neo}$ mice showed attenuation of PNKP levels (Fig 6B). Thus, similar to MCSZ in humans, $Pnkp^{Neo/Neo}$ mice contained germ line attenuation of PNKP expression. In contrast to complete *Pnkp* deletion or homozygous expression of the *MCSZ* allele, $Pnkp^{Neo/Neo}$ mice were viable and demonstrated neurodevelopmental deficits associated with reduced overall PNKP levels (Fig 6; Appendix Fig S4). While the reduced PNKP levels resulted in a smaller brain (see Fig 6B, arrows), analogous to that found in the human MCSZ syndrome, they were also associated with generalized growth defects. Thus, the relative impact of reduced *Pnkp* expression in mouse is more consequential than in humans. Nonetheless, these mice are valuable for understanding the physiologic requirement for PNKP during neural development.

Similar to $Pnkp^{Nes\text{-}cre}$ mice, we found substantial apoptosis in the $Pnkp^{Neo/Neo}$ brain from E13.5 that accounted for the smaller organ size (Fig 6C). Analysis of the developing E13.5 $Pnkp^{Neo/Neo}$ neocortex showed an increase in DNA damage (γH2AX) and associated apoptosis (TUNEL) in mutant tissue compared to controls (Fig 6C). There was a concomitant reduction in proliferating cells (phosphohistone H3) in both the apical and basal progenitor populations in the $Pnkp^{Neo/Neo}$ tissue (Fig 6C, arrows), as proliferating cells are susceptible to DNA damage-induced apoptosis.

We also determined DNA repair capacity in primary cells isolated from the hypomorphic $Pnkp^{Neo/Neo}$ mice to compare with repair defects associated with reduced PNKP levels found in MCSZ (Shen *et al*, 2010; Reynolds *et al*, 2012). Because the $Pnkp^{Neo/Neo}$ alleles are expressed in the germ line, we examined $Pnkp^{Neo/Neo}$ mouse embryonic fibroblasts (MEFs) after various genotoxins (Fig 6D). We found reduced chromosomal DNA repair capacity in $Pnkp^{Neo/Neo}$ MEFs compared to WT controls. Notably, we found some differential sensitivity to genotoxins, as the $Pnkp^{Neo/Neo}$ MEFs were more defective in repair of IR or MMS damage compared with CPT; this was apparent in comparison with the $Lig4^{-/-}$ and $Tdp1^{-/-}$ mutants that were used as positive (repair-deficient) controls, and probably relates to the relative requirements for PNKP in different end-processing events (Fig 6D). We also used neutral comet assays to measure DNA DSBs after IR or bleomycin and found comparable DNA repair defects in $Pnkp^{Neo/Neo}$ cells to those present in Lig4-null cells, further illustrating defective DSBR after compromised PNKP levels (not shown). These data suggest that reduced PNKP levels in the $Pnkp^{Neo/Neo}$ mice create a scenario much like that in MCSZ, where PNKP levels are sufficient for viability, but compromise

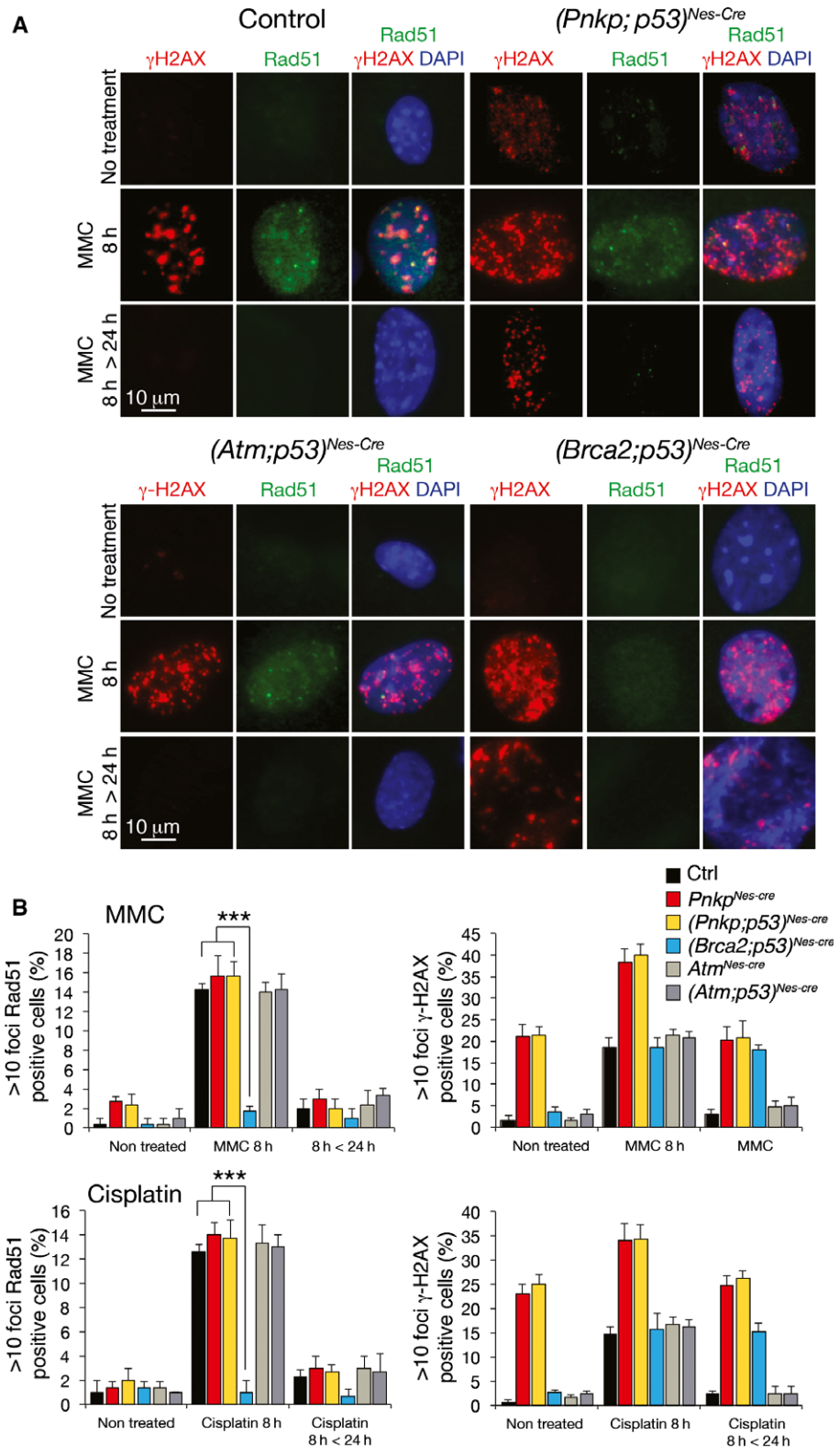


**Figure 5. PNKP is dispensable for DNA repair by homologous recombination.**

A Homologous recombination (HR) after mitomycin C (MMC) exposure was monitored in primary astrocytes lacking PNKP, BRCA2 or ATM by recovery of damage-induced γH2AX and RAD51 foci utilizing immunocytochemistry. In contrast to PNKP deficiency, cells deficient in the HR factor BRCA2 have a measurable deficit in DNA repair after MMC, while ATM-null cells do not show defective HR.

B Quantitation of repair and recovery of γH2AX and RAD51 foci in (A) is shown graphically. The mean (± SD) is from at least 3 replicates. ***$P < 0.003$.

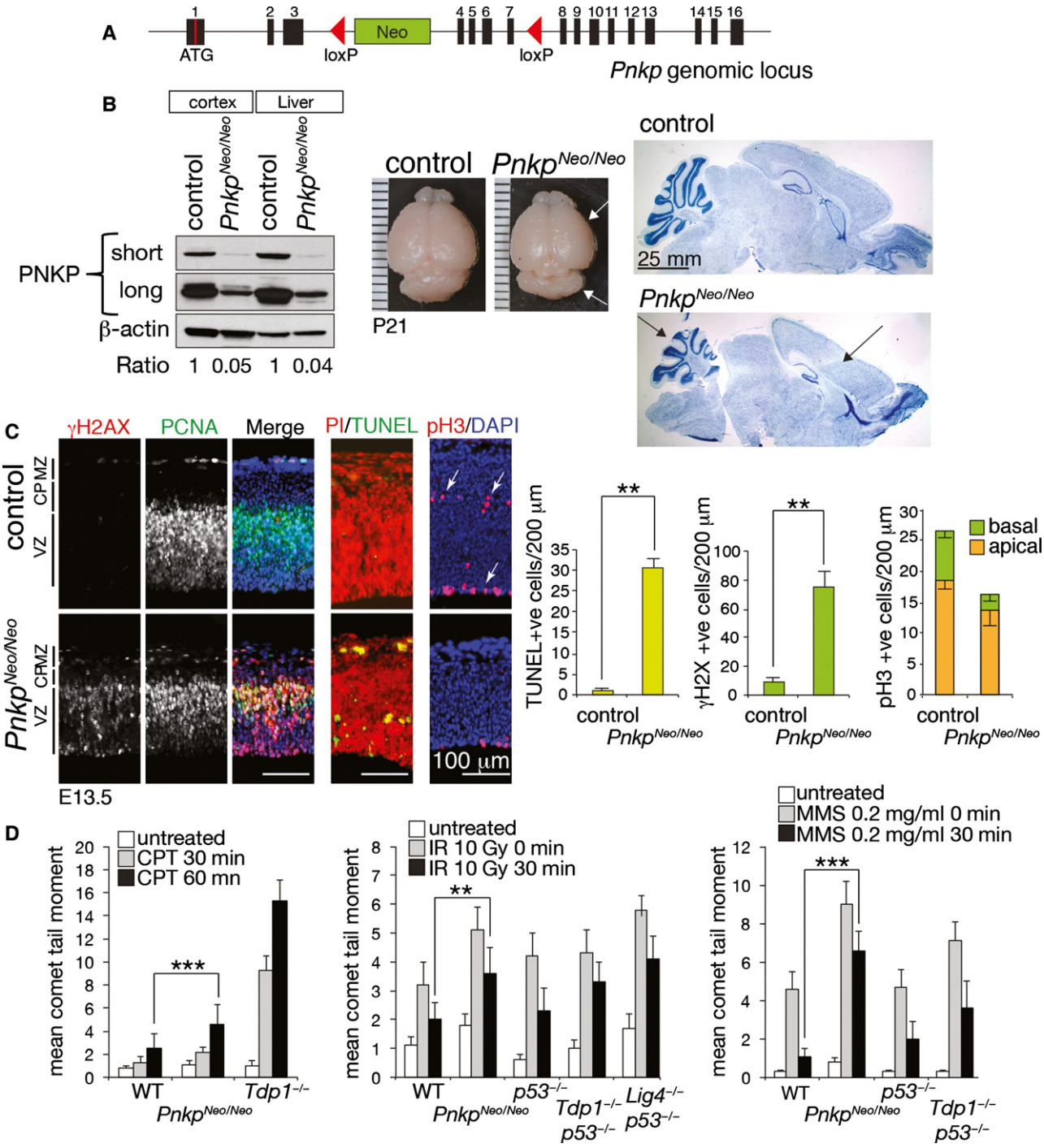


**Figure 6. A hypomorphic germ line *Pnkp* allele with attenuated PNKP levels impacts development and DNA repair.**

A A neomycin selection cassette (Neo) was inserted in intron 4 to generate the $Pnkp^{Neo}$ allele.

B Western blot analysis shows that the $Pnk^{Neo/Neo}$ allele attenuates PNKP levels. Shorter and longer exposure show relative PNKP levels in the $Pnkp^{Neo/Neo}$ tissue; the ratio of protein levels in the *Pnkp* mutant compared with controls is shown below the blots. Overall brain size is mildly affected compared to complete PNKP inactivation (arrows in photograph and Nissl-stained sagittal cryosections).

C Attenuated PNKP level is associated with an increase in DNA damage formation (γH2AX) and apoptosis (TUNEL), and reduced immunostaining of the proliferation markers PCNA and pH3. Arrows indicate the basal and apical cortical progenitors. Adjacent graphs quantify DNA damage, apoptosis and proliferation. The mean (± SD) is from at least 3 replicates. $^{**}P < 0.009$.

D Quiescent primary mouse embryonic fibroblasts (MEFs) from $Pnkp^{Neo/Neo}$ embryos also show a DNA repair defect after camptothecin (CPT) as determined using alkaline comet assays. Repair of ionizing radiation (IR) and methyl methanesulfonate (MMS) is also defective in $Pnkp^{Neo/Neo}$ proliferating MEFs as determined using alkaline comet assays. $Tdp1^{-/-}$ and $(Lig4;p53)^{-/-}$ MEFs were also used as a positive control for defective DNA repair. The mean (± SD) is from at least 3 replicates. $^{***}P < 0.0001$, $^{**}P < 0.005$.

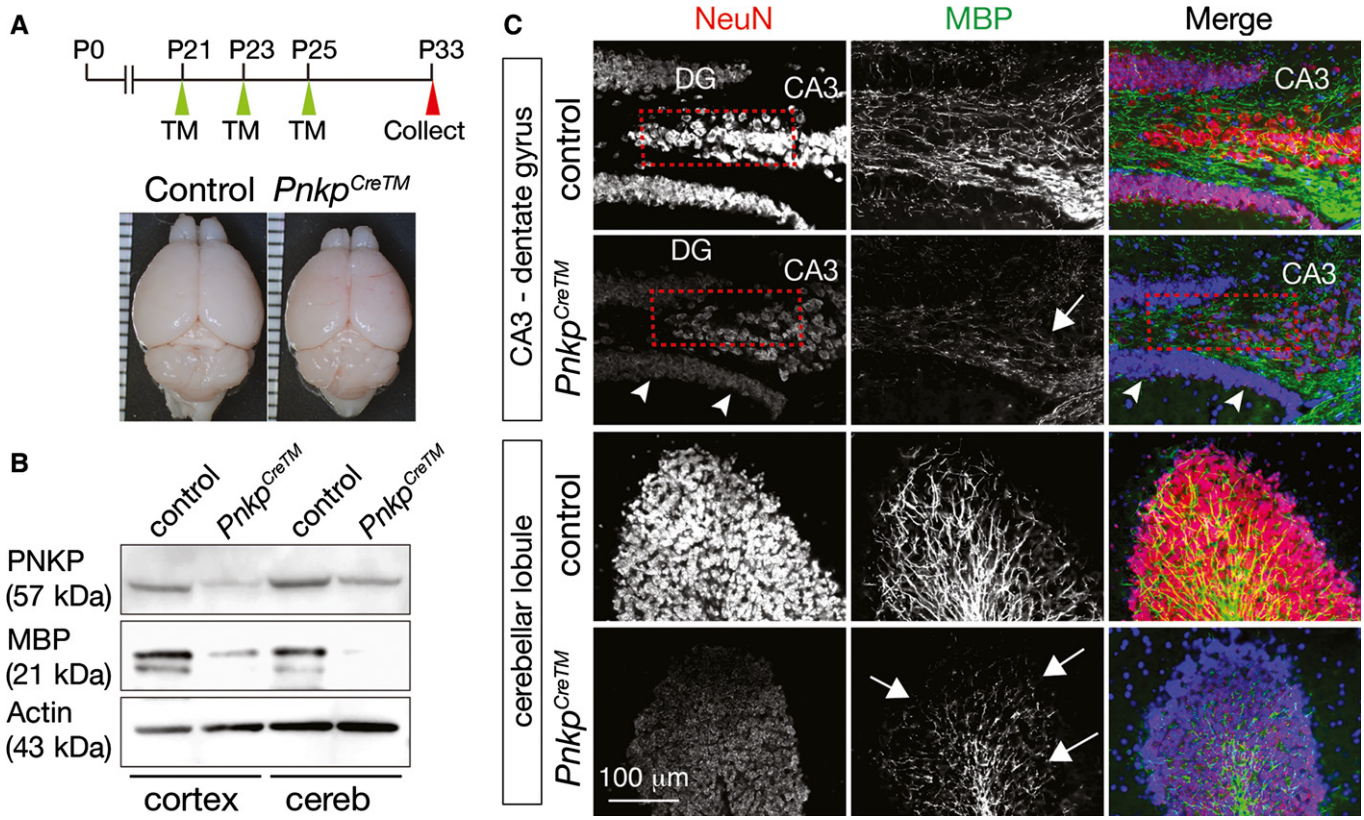


**Figure 7. Induced *Pnkp* deletion in the postnatal brain affects multiple cell types.**

A Inducible *Pnkp* deletion commencing at postnatal day 21 (P21) using a tamoxifen (TX)-inducible actin-based promoter reveals little overall effect toward brain size or structure.

B Western blot analysis shows reduced PNKP levels after *CreTM* induction in multiple brain regions. There is also a reduction of myelin basic protein (MBP) in the $Pnkp^{CreTM}$ brain. Actin serves as a loading control.

C Analysis of the $Pnkp^{CreTM}$ brain after TX administration using the neuronal marker NeuN, which immunostains mature neurons, revealed a marked reduction of this marker in the dentate gyrus (DG) and the hippocampal CA3 region (red-hatched boxes), and the cerebellum. The myelin-producing oligodendrocytes also show a reduction in myelination as judged by reduced MBP immunostaining (arrows), consistent with reduced protein levels in (B). Arrowheads indicate that although NeuN immunostaining is decreased in the mutant, this is not due to cell loss as seen in the DAPI-stained merged image.

genome integrity in the face of endogenous DNA lesions, leading to neural cell loss and resultant neuropathology.

### PNKP maintains differentiated neurons

Little is known regarding the ongoing requirement for DNA repair factors in differentiated neural populations after the completion of neurogenesis (McKinnon, 2013). However, this is likely to be important for neural homeostasis, and to prevent progressive decline observed in many DNA repair deficiency syndromes. Therefore, we generated mice in which a tamoxifen (TX)-inducible promoter was used for *Pnkp* inactivation in different neural compartments after neurogenesis. We initially examined the effect of postnatal *Pnkp* deletion using CreTM, an actin-based promoter that is effective for broad neural gene inactivation (Hayashi & McMahon, 2002). We induced deletion at P21 using TX (a dose every 2 days, for a total of 3 doses) and examined tissue approximately 2 weeks later (Fig 7A). Compared to $Pnkp^{Nes\text{-}cre}$ animals, TX treatment had a relatively modest effect toward the $Pnkp^{CreTM}$ brain, with little discernable gross tissue effect (Fig 7A). This lack of an overt effect after PNKP loss is likely because cells were non-replicative, thereby avoiding apoptosis from DNA damage during proliferation.

Inactivation of PNKP was confirmed using Western blot analysis, which showed reduced PNKP levels in TX-treated $Pnkp^{CreTM}$ brain tissue (Fig 7B). Under the induction conditions used, effective PNKP loss occurred throughout the cortex, while loss was more modest throughout the cerebellum. When cre induction began at earlier stages such as P7, the overall consequences of PNKP inactivation were more pronounced, in accord with increased neurogenesis at this earlier time (Appendix Fig S5). Nonetheless, deleterious effects of *Pnkp* inactivation toward multiple neural cell types were observed by P33 after TX administration at P21 (Fig 7C). For example, myelin basic protein (MBP), a central component for myelination by oligodendrocytes (Emery, 2010), was found to be markedly reduced throughout the $Pnkp^{CreTM}$ brain, by both immunostaining and Western blot analysis (Fig 7B and C). Additionally, we found that the level of NeuN, an RNA splicing factor (Kim *et al*, 2009) also known as Fox-3, which is expressed in mature neurons, was strongly attenuated (Fig 7B). To investigate whether the reduction in MBP is associated with oligodendrocyte loss, we used Sox10,

 

which is a specific marker of oligodendrocytes in the central nervous system (Stolt *et al*, 2002). We found that numbers of Sox10-positive cells were similar between control and the TX-induced $Pnkp^{CreTM}$ cortex, although there was a reduction in cell numbers in the dentate gyrus, a structure that maintains neurogenesis until ~P36 (Appendix Fig S6). Similarly, the observed NeuN decrease was not associated with loss of neurons as evident by similar DAPI staining between control and mutant tissues (Fig 7C, white arrowheads). These data indicate a broad impact of PNKP inactivation throughout the postmitotic brain, although not involving overt cell loss as found during neurogenesis. In contrast, *Pnkp* deletion after TX treatment between P7 and P14, when neurogenesis is still occurring in the dentate gyrus and cerebellum, showed a more pronounced effect involving neurogenesis-associated cell loss (Appendix Fig S7). Again, we also found a clear effect of PNKP loss toward oligodendrocytes, with a reduction in MBP by P20 after induction of *Pnkp* inactivation at P7 (Appendix Fig S6). Thus, the genome maintenance functions of PNKP are critical for the homeostasis and survival of postnatal neural populations.

### PNKP is an essential factor for glial homeostasis

Based on the oligodendrocyte sensitivity data above, and because the relative *in vivo* requirements for the DDR in glial cells are unclear, we used an inducible *GFAP-cre* promoter (Chow *et al*, 2008) to generate $Pnkp^{Gfap\text{-}creTM}$ mice to further assess PNKP in selective neural compartments. *GFAP-creTM* is a transgene that directs cre expression throughout glia in the adult brain, but with only sporadic expression in the radial glia progenitors in the subventricular zone progenitors of the lateral ventricle, thereby mostly restricting gene deletion to differentiated glia (Chow *et al*, 2008).

We found that even with early deletion at P1, the loss of PNKP in $Pnkp^{Gfap\text{-}creTM}$ produced a less severe phenotype than $Pnkp^{CreTM}$ (Appendix Fig S5), with overall brain and body size being similar to controls, although a modest reduction in cortical size was found in $Pnkp^{Gfap\text{-}creTM}$ brains (Fig 8A). We again observed an oligodendrocyte defect in $Pnkp^{Gfap\text{-}creTM}$ mice as determined by decreased immunostaining for MBP (Fig 8B). We also observed altered NeuN immunostaining patterns in cortical neurons, which given the lack of neuronal expression of the *GFAP-creTM* transgene, likely reflect an indirect effect from loss of myelination (Fig 8B). Other markers of oligodendrocytes such as MBP, 2′,3′-cyclic-nucleotide 3′-phosphodiesterase (CNPase) and Olig2 are also affected by PNKP inactivation (Fig 8C). These effects did not involve oligodendrocyte cell loss, as Sox10 immunopositive cell numbers were similar between $Pnkp^{Gfap\text{-}creTM}$ and control brains (Fig 8D). In contrast to oligodendrocytes, loss of astrocytes was found in $Pnkp^{Gfap\text{-}creTM}$ brain, reflecting ongoing proliferation in these cells (Appendix Fig S8). Collectively, our data indicate that attenuated PNKP levels cause pronounced neuropathology, which is characterized by retarded neural development and microcephaly resulting from DNA damage during neurogenesis. PNKP also fulfills important genome maintenance functions after the completion of neurogenesis to preserve neural homeostasis, as loss of PNKP strongly impacts oligodendrocytes, which may account for white matter abnormalities that are apparent as disease progression occurs in MCSZ (Poulton *et al*, 2013).

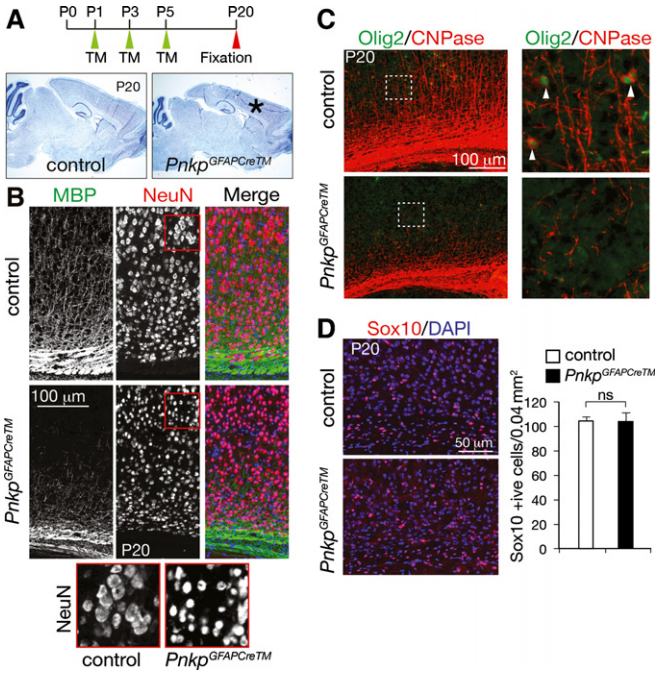


**Figure 8. PNKP is an essential maintenance factor for glia in the postnatal brain after neurogenesis.**

A Selective inactivation of *Pnkp* in the glia using *GFAP-creTM* reveals an important role for PNKP function in maintaining these neural cells. *Pnkp* deletion at P1 results in a brain with mild cortical and cerebellar size reduction (asterisk).

B Myelin basic protein immunostaining is strongly reduced by P20 in the $Pnkp^{GFAP\text{-}creTM}$ brain after induction at P1. NeuN (Fox-3) immunostaining also reveals alteration in nuclear morphology, likely as an indirect consequence of PNKP inactivation in glia.

C $Pnkp^{GFAP\text{-}creTM}$ broadly impacts oligodendrocytes as CNPase and Olig2 immunostaining are also reduced.

D Alteration in MBP, CNPase and Olig2 does not involve loss of oligodendrocytes as revealed by normal numbers of Sox10-positive cells. Graph shows quantitation of oligodendrocyte cell bodies (Sox10) in the control and $Pnkp^{GFAPCreTM}$ cortex. The mean (± SD) is from at least 3 sections. ns, not significant.

## Discussion

The MCSZ phenotype results from germ line *PNKP* mutations and extensively affects the nervous system. Given the ubiquitous tissue distribution of the BER pathway, this essential neural function of PNKP implicates increased levels or specific types of endogenous DNA lesions (e.g., those arising from oxidative damage), possibly coupled to a lower threshold of cellular tolerance in this tissue. To determine how PNKP maintains genome integrity in the setting of the nervous system, we adopted a multipronged approach to understand the functional relevance of this enzyme to neural homeostasis and disease. Here we provide a comprehensive analysis of the *in vivo* physiologic role of PNKP during development. Our data showed that the MCSZ phenotype is attributable to endogenous DNA damage and reduced repair capacity because of decreased PNKP levels, resulting in neural cell death and microcephaly. Furthermore, we also show that there is an ongoing role for PNKP function after the completion of neurogenesis, which is critical in the

glial cell population. Thus, our data demonstrate that reduced PNKP function in the face of endogenous DNA damage widely impacts the nervous system resulting in a phenotype reflective of MCSZ.

In other neurologic syndromes, loss of SSBR factors leads to neurodegeneration without extra-neurologic consequences, while deficiency in DNA DSBR results in neurodegeneration or microcephaly associated with broad defects throughout the body (McKinnon, 2009, 2013). While PNKP is a key factor in BER via its interaction with the SSBR factor XRCC1, it has also been shown to associate with XRCC4, a factor involved in the NHEJ pathway that repairs DNA DSBs, thereby implicating PNKP in both SSBR and DSBR (Koch *et al*, 2004; Caldecott, 2008). Our data clearly show a role for PNKP in both BER and NHEJ (but not HR) consistent with prior reports involving cell reconstitution studies and RNA interference experiments (Chappell *et al*, 2002; Koch *et al*, 2004; Karimi-Busheri *et al*, 2007). However, as the repair defects found in $Pnkp^{-/-}$ cells after IR are similar to those seen after XRCC1 or LIG4 loss rather than being substantially greater, it is likely that PNKP may participate in a fraction of the breaks during NHEJ repair of IR damage, rather than all breaks as would be expected for LIG4. Given the importance for PNKP during both BER and NHEJ, one would predict deficiency of this factor would impact outside the nervous system similar to human syndromes characterized by DSBR defects such as Nijmegen breakage syndrome or Lig4 syndrome (Girard *et al*, 2004; Ben-Omran *et al*, 2005; O'Driscoll & Jeggo, 2006). This may indicate that in MCSZ, specific types of abundant neural DNA lesions (arising from high oxygen consumption?) depend on normal PNKP levels, compared to other general DNA lesions.

In contrast to the human disease, the observation that our engineered mouse MCSZ mutation is incompatible with embryo viability suggests that different thresholds exist for PNKP function between human and mouse. However, phenotypic variation exists in humans harboring the T424GfsX48 allele; although the MCSZ phenotype is microcephaly (Shen *et al*, 2010), this allele was recently linked to neurodegeneration and cerebellar ataxia in another family with two affected siblings (Poulton *et al*, 2013). Thus, these phenotypic differences in human MCSZ may suggest genetic modifiers or background can affect the outcome of PNKP inactivation. Possibly, the mouse strains used in our study predispose to higher sensitivity to PNKP loss?

We also identified an ongoing requirement for PNKP function in mature neuronal and glial cells, by inducing gene deletion after the cessation of neurogenesis. Inactivation of PNKP in non-cycling SOX10-positive oligodendrocytes led to loss of myelination, indicating endogenous DNA damage impacts mature glial function. As oligodendrocytes are sensitive to oxidative stress (Dewar *et al*, 2003; Jana & Pahan, 2007; French *et al*, 2009), this may indicate a key role for PNKP for DNA repair of oxidative DNA damage. PNKP requirement in glia is also notable in light of a report indicating that glia do not activate a DNA damage response (Schneider *et al*, 2012). We have previously shown that glia do activate a normal DDR if their genome integrity is compromised (Lee *et al*, 2012a, 2014). DNA damage-induced disruption of normal oligodendrocyte function may well underpin white matter defects typical of MCSZ (Shen *et al*, 2010; Poulton *et al*, 2013). In fact, this sensitivity of oligodendrocytes raises the possibility that genomic damage and genotoxins may contribute to demyelination defects in more common neurologic disease such as multiple sclerosis (MS) (Lee *et al*, 2012b). This is particularly relevant as oligodendrocyte turnover in humans is very limited, while myelination changes are dynamic and contribute to neural plasticity (Yeung *et al*, 2014). Importantly, as the initiating lesions that underpin MS are relatively unknown (Lassmann *et al*, 2012; Friese *et al*, 2014), links between genome damage and white matter/myelin defects warrant closer inspection.

In the case of neurons, we found a marked attenuation of NeuN levels (an RNA splicing factor expressed in mature neurons), indicating neural homeostasis is perturbed. However, given that we found an effect on NeuN-positive neurons after *Pnkp* deletion via *Gfap-creTM*, glial defects may contribute more broadly in the mature brain to ongoing neuropathology. The oligodendrocyte/MBP sensitivity, and altered NeuN expression, suggests that disease progression may also involve disruption of transcription as a consequence of DNA damage. Transcription-associated R-loops are potential sources of DNA breaks that can compromise genome stability, highlighting the need for DNA repair in this setting (Mischo *et al*, 2011; Aguilera & Garcia-Muse, 2012; Gaillard *et al*, 2013; Bhatia *et al*, 2014). Transcriptional disruption has been suggested to underpin the neurodegenerative phenotype associated with AOA2, SCAN1 and other neurologic diseases resulting from genomic damage (Suraweera *et al*, 2009; King *et al*, 2013; Richard *et al*, 2013; Yuce & West, 2013; Gomez-Herreros *et al*, 2014).

Thus, PNKP is an essential DNA repair factor that participates in both DSBR and SSBR, and is necessary to prevent severe neurologic decline in humans. Our data indicate that genome stability afforded by PNKP is critical both during neurogenesis and in the mature brain. These findings point to the ongoing need for multiple genome stability mechanisms at all stages of the nervous system, underscoring the critical links between genome stability and the prevention of neurologic disease.

## Materials and Methods

### *Pnkp* mutant mice

Two individual targeting vectors were constructed to generate a conditional *Pnkp* allele or the *MCSZ* mutant allele. The *Pnkp* conditional strategy resulted in exons 4–7 flanked by *LoxP* sites. To achieve this, we used recombineering to introduce a single *LoxP* site between exons 7 and 8 and a neomycin selection cassette flanked by *Frt* sites with a single *LoxP* site was inserted between exons 3 and 4. The targeting construct was electroporated into W9.5 embryonic stem (ES) cells, and after selection with G418, homologous recombinants were screened by Southern blotting using both 3′ and 5′ probes outside the targeted region. Positive clones were blastocyst-injected to generate chimeric mice. The male chimeras were bred with C57BL/6 females to establish mice carrying the targeted *Pnkp* allele. The initial mouse line still contained the neomycin cassette inserted in intron between exons 3 and 4, $Pnkp^{Neo}$. Because the homozygous $Pnkp^{Neo/Neo}$ mice had a significant phenotype, they were maintained as an independent line (this mutation was germ line; therefore, these mice were not crossed with cre lines). Further breeding with *Flp* recombinase mice (JAX #003800: B6; SJL-TG (ACTFLPE)9205 DYM/J) removed the neomycin cassette resulting in the conditional $Pnkp^{loxP}$ line.

 

Further breeding with cre mice under the control of the Nestin promoter (JAX #003771: B6.Cg-Tg(Nes-cre)1Kln/J) resulted in deletion throughout the nervous system (http://cre.jax.org/Nes/Nes-Cre Nano.html), while breeding with the *Emx1-cre* mice (JAX #005628; B6.129S2-*Emx1*$^{tm1(cre)Krj}$/J) deleted *Pnkp* in Emx1-expressing neural progenitors. *Sox2-cre* mice (JAX #004783; Tg(Sox2-cre)1Amc) were used to delete *Pnkp* in the embryo proper (avoiding placental inactivation). CreTM (JAX #004682; B6.Cg-Tg (CAG-cre/Esr1)5Amc/J), Rosa26CreTM (JAX 008463: B6. 129-Gt (ROSA) 26Sor$^{tm1(cre/ERT2)Tyj/J)}$ and *GFAP-CreTM*$^{ER2}$ (Chow *et al*, 2008) provided tamoxifen-inducible cre expression driven from the actin or *GFAP* promoter, respectively, and were used to obtain primary cell cultures.

The MCSZ mutant mice were created using recombineering; an initial targeting introduced the 17-bp mutation into exon 13 leaving a *LoxP* site in the preceding intron (between exons 12 and 13). The neomycin–thymidine kinase dual selection cassette flanked by *Frt* sites with a single *LoxP* was inserted between exons 3 and 4. A second round of selection in ES culture following transfection with Flp recombinase and using FIAU resulted in a clone which was subsequently injected into blastocysts and the resulting chimeric males bred with C57BL/6 females to establish mice carrying the mutant *Pnkp* allele.

Other mice used were *p53*$^{LoxP}$, *Atm*$^{LoxP}$, *Lig4*$^{LoxP}$ and *Xrcc1*$^{LoxP}$ which have been described previously (Herzog *et al*, 1998; Lee *et al*, 2009; Shull *et al*, 2009). The *Atm* conditional allele was engineered to have exon 58 flanked by *LoxP* sites (Lee *et al*, 2012a). All animal experiments were carried out according to NIH regulations and were approved by the SJCRH Animal Care and Use Committee.

#### Tamoxifen-induced cre expression

Tamoxifen administration was done via intraperitoneal injection using tamoxifen (Sigma) dissolved in corn oil (Sigma) at 10 mg/ml. Tamoxifen injections were done with *Pnkp*$^{Rosa\text{-}CreTM}$, *Pnkp*$^{CreTM}$, *Pnkp*$^{Gfap\text{-}CreTM}$ and *Xrcc1*$^{Rosa\text{-}CreTM}$ mice using a dose of 1 mg/10 g mouse body weight as per the indicated dosing schedules.

#### Histology and immunodetection

Mice underwent transcardial perfusion with 4% (w/v) buffered paraformaldehyde (PFA), or embryos were drop-fixed in 4% PFA. Brains or embryos were cryoprotected in buffered 25% sucrose (w/v) solution. After embedding in Tissue-Tek OCT compound (Sakura), samples were cryosectioned sagittally at 10 μm using a CM3050S cryostat (Leica). Immunohistochemical analysis of sectioned samples was first subjected to antigen retrieval according to the manufacturer's directions (HistoVT One, Nacalai Tesque). For all immunohistochemistry and immunocytochemistry, the following antibodies (in alphabetical order) were used: 53BP1 (rabbit, 1:500, Bethyl Labs, cat# A300-272A), Brn2 (rabbit, 1:200, Gene-Tex, cat# GTX114650), CNPase (mouse, 1:500, Sigma, cat# C5922), Ctip2 (rat, 1:100, Abcam, cat# ab18465), Cux1 (CDP, rabbit 1:100 Santa Cruz, cat# SC13024), GFAP (mouse, 1:500, Sigma, cat# G3893), γH2AX (Ser139, rabbit, 1:500, Cell Signaling, cat# 2577, and mouse, 1:500, Millipore, cat# 05-636), phospho-histone H3-Ser10 (mouse, 1:1,000, Cell Signaling, cat# 9706S), MBP (rabbit, 1:500, Abcam, cat# ab40390), NeuN (mouse, 1:500, Chemicon, cat# MAB377), Olig2 (rabbit, 1:500, Millipore, cat# AB9610), Pax2 (rabbit, 1:500, Zymed, cat# 71-6000) PCNA (clone PC10, mouse, 1:500, Santa Cruz, cat# SC-56), RAD51 (rabbit, 1/500, Santa Cruz, cat# sc8349), Satb2 (mouse, 1:50, Abcam, cat# 51502), Sox2 (rabbit, 1:500, Millipore, cat# AB5603), Sox10 (rabbit, 1:250, Abcam, cat# ab155279), Tbr1 (rabbit, 1:100, Abcam, cat# ab31940) and Tuj1/β-tubulin III (mouse, 1:1,000, Covance, cat# MMS-435P). For colorimetric visualization of positive signals, sections were incubated with primary antibodies overnight at room temperature, and endogenous peroxidase was quenched using 0.6% (v/v) $H_2O_2$ in methanol and blocked with goat serum [5% (v/v) goat serum, 1% (w/v) BSA in PBS-T] at room temperature for 1 h. Slides were washed three times with PBS followed by a 1-h incubation with biotinylated secondary antibody and avidin–biotin complex (Vectastain Elite kit, Vector Labs). Immunoreactivity was visualized with the VIP substrate kit (Vector Labs) using the manufacturer's protocol. Sections were counterstained with 0.1% (w/v) methyl green, dehydrated and mounted in DPX (Fluka). For fluorescent detection of immunoreactivity, FITC- or Cy3-conjugated secondary antibodies (Jackson Immunologicals) were used and counterstained with 4′,6-diamidino-2-phenylindole (DAPI; Vector Laboratories).

For BrdU incorporation assays, pregnant mice at E13.5 or E15.5 were injected (60 μg per 1 g of body weight), and 2 h after injection, embryos were drop-fixed in 4% PFA and processed for cryosectioning and anti-BrdU (rat, 1:200, Abcam, cat# ab6326-250) immunostaining was assessed. Apoptosis was measured by TUNEL assay using Apoptag (Millipore) according to the manufacturer's protocol. Following TUNEL staining, sections were counterstained with propidium iodide (PI) in mounting medium (Vector Laboratories). Nissl staining was performed with 1% (w/v) thionin using standard protocol; Hematoxylin/eosin staining was also performed using standard procedures.

#### Isolation of primary cells and immunofluorescence

Primary astrocytes were prepared from P1 to P5 mouse brains as described previously (Katyal *et al*, 2007). Cortices were dissected free of meninges and then dissociated by passage through a 5-ml pipette, and cells were resuspended in Dulbecco's modified Eagle's medium and Ham's nutrient mixture F-12 (1:1 DMEM/F12, Gibco-BRL) supplemented with 10% fetal bovine serum (v/v), 1× glutamax, 100 U/ml penicillin, 100 mg/ml streptomycin and 20 ng/ml epidermal growth factor (EGF; Millipore). Primary astrocytes were established and maintained in Primaria T-25 tissue culture flasks (Falcon) at 37°C in a humidified $CO_2$-regulated (5%) incubator.

Primary MEFs were prepared from E13.5 embryonic mesenchyme. Tissue was minced using dissection scissors, trypsinized and resuspended in Dulbecco's modified Eagle's medium supplemented with 10% fetal bovine serum (v/v), 1× glutamax, 100 U/ml penicillin, 100 μg/ml streptomycin and β-mercaptoethanol and established in T-25 tissue culture flasks (Falcon) at 37°C in a humidified $CO_2$-regulated (5%) incubator.

For fluorescent labeling of quiescent cortical astrocytes or MEFs, cells were grown to confluence on glass coverslips, fixed with 4% PFA in PBS for 10 min and permeabilized for 5 min in 0.5% Triton X-100/PBS. Cells were immunostained as described above, followed by Alexa 488/555-conjugated secondary antibodies and counterstained with DAPI.

#### Alkaline comet assay

Cells were treated with either 150 μM $H_2O_2$ (Thermo Fisher) on ice for 5 min, methyl methanesulfonate (MMS, Sigma) for 10 min at 0.2 mg/ml at 37°C, 14 μM camptothecin (CPT, Calbiochem) at 37°C for 30 or 60 min, bleomycin (Bedford Laboratories) at 40 μg/ml for 30 at 37°C, or γ–irradiation (10 Gy for alkaline comet assay or 20 Gy for neutral comet assay using $^{137}Cs$). After this step, all subsequent steps were performed in the dark, and comet assays were done as previously described (Katyal *et al*, 2007, 2014). Briefly, trypsinized cells were mixed with equal volume of 1.2% low-melting-point agarose (Invitrogen) and plated onto frosted glass slides (Fisher) pre-coated with 0.6% agarose. Slides were treated with lysis buffer (2.5 M NaCl, 10 mM Tris–HCl, 100 mM EDTA (pH 8.0), 1% Triton X-100, 3% DMSO, pH 10) for 1.25 h at 4°C and placed in pre-chilled alkaline electrophoresis buffer (50 mM NaOH, 1 mM EDTA and 1% DMSO) for 45 min. Electrophoresis was done at 95 mA for 25 min and neutralized in 0.4 M Tris–HCl (pH 7.5). Comets were stained using SYBR Green (1:10,000 in 0.4 M Tris–HCl, pH 7.5) for 10 min. At least 100 comets/experiment were counted and measured using the Comet Assay IV system (Perceptive Instruments) together with an Axioskop2 plus microscope (Carl Zeiss) at ×200 magnification.

#### Neutral comet assay

Neutral comet assays were done as above, but using a sodium acetate-based electrophoresis buffer (300 mM NaOAc, 100 mM Tris–HCl, pH 8.5); electrophoresis was performed with at 190 mA for 50 min followed by washing in neutralization buffer (0.4 M Tris–HCl pH 7.5).

#### Western blotting

Mouse tissues were harvested and extracted by RIPA buffer (0.1 M Tris–HCl (pH 7.5), 0.5 M NaCl, 0.05 M EDTA, 1% Triton X-100, 1% SDS, 1% sodium deoxycholate) with protease inhibitors (1 mM NaF, 1 mM $Na_3VO_4$, protease inhibitor cocktail (Roche)). Proteins were quantified using Bradford standard method (Bio-Rad). Protein samples were electrophoresed with 4–12% Bis-Tris SDS–polyacrylamide gel (Invitrogen) and transferred to nitrocellulose membrane (Bio-Rad). Membranes were blocked by 5% skim milk/TBS-T at 37°C for 1 h. Primary antibody was incubated at room temperature for 4–24 h. Antibodies used for Western blotting were as follows: β-actin (goat, 1:1,000, Santa Cruz, cat# sc1616), MBP (rabbit, 1:2,000, Abcam, cat# ab40390), NBS1 (rabbit, 1:1,000, Cell Signaling, cat# 3002) and PNKP (rabbit, 1:1,000, Novus, cat# NBP1-87257). Secondary antibody was reacted at room temperature for 1 h. Membranes were developed using Amersham ECL Western blotting detection reagent (GE Healthcare Life Sciences). Ponceau S staining was used as a loading control.

#### Magnetic resonance imaging (MRI)

$Pnkp^{Nes\text{-}Cre}$, $Pnkp^{Neo/Neo}$ and control mice (age at P2 and 8 months, respectively, sex matched) were used for MRI analysis. All scans were performed with 7 Tesla Bruker Clinscan animal magnetic resonance imaging scanner (Bruker Biospin MRI GmbH).

#### *In situ* cell counts

To determine γH2AX, BrdU, phospho-H3 or TUNEL-positive cell numbers in E13.5 and E15.5 embryonic cortex, immunostained sections were subjected to quantitative analysis. Three embryos for each genotype were analyzed. Immunopositive signals were measured within 200-μm fields from at least three representative sections of the neocortex for each individual embryo.

#### Statistical analysis

Unpaired Student's *t*-tests were used for the determination of *P*-values. Values represented the mean and standard error of at least three independent experiments.

**Expanded view** for this article is available online:
http://emboj.embopress.org


### Acknowledgements
We thank Dr. Suzanne Baker for providing the GFAP-creTM mice and Susanna Downing for helpful comments and advice. We also thank Dr. Jingfeng Zhao and Yang Li for genotyping and technical help. We thank the Animal Resource Center, the Small Animal Imaging Center and the Transgenic Core Unit for support with mouse work. PJM is supported by the NIH (NS-37956, CA-21765), the CCSG (P30 CA21765) and the American Lebanese and Syrian Associated Charities of St. Jude Children's Research Hospital. MS is also supported by the Uehara Memorial Foundation of Life Sciences.


### Author contributions
MS and PJM conceived and planned all project experiments and produced the final version of the manuscript. MS and LCD performed all experiments. HRR generated the *Pnkp* mutant mouse models and helped with experiments.

### Conflict of interest
The authors declare that they have no conflict of interest.

## References


Aguilera A, Garcia-Muse T (2012) R loops: from transcription byproducts to threats to genome stability. *Mol Cell* 46: 115 – 124

Ahel I, Rass U, El-Khamisy SF, Katyal S, Clements PM, McKinnon PJ, Caldecott KW, West SC (2006) The neurodegenerative disease protein aprataxin resolves abortive DNA ligation intermediates. *Nature* 443: 713 – 716

Almeida KH, Sobol RW (2007) A unified view of base excision repair: lesion-dependent protein complexes regulated by post-translational modification. *DNA Repair* 6: 695 – 711

Ben-Omran TI, Cerosaletti K, Concannon P, Weitzman S, Nezarati MM (2005) A patient with mutations in DNA Ligase IV: clinical features and overlap with Nijmegen breakage syndrome. *Am J Med Genet A* 137A: 283 – 287

Bhatia V, Barroso SI, Garcia-Rubio ML, Tumini E, Herrera-Moyano E, Aguilera A (2014) BRCA2 prevents R-loop accumulation and associates with TREX-2 mRNA export factor PCID2. *Nature* 511: 362 – 365

Breslin C, Caldecott KW (2009) DNA 3′-phosphatase activity is critical for rapid global rates of single-strand break repair following oxidative stress. *Mol Cell Biol* 29: 4653 – 4662

Caldecott KW (2008) Single-strand break repair and genetic disease. *Nat Rev Genet* 9: 619 – 631

Chappell C, Hanakahi LA, Karimi-Busheri F, Weinfeld M, West SC (2002) Involvement of human polynucleotide kinase in double-strand break repair by non-homologous end joining. *EMBO J* 21: 2827 – 2832

Chow LM, Zhang J, Baker SJ (2008) Inducible Cre recombinase activity in mouse mature astrocytes and adult neural precursor cells. *Transgenic Res* 17: 919 – 928

Date H, Onodera O, Tanaka H, Iwabuchi K, Uekawa K, Igarashi S, Koike R, Hiroi T, Yuasa T, Awaya Y, Sakai T, Takahashi T, Nagatomo H, Sekijima Y, Kawachi I, Takiyama Y, Nishizawa M, Fukuhara N, Saito K, Sugano S *et al* (2001) Early-onset ataxia with ocular motor apraxia and hypoalbuminemia is caused by mutations in a new HIT superfamily gene. *Nat Genet* 29: 184 – 188

Deans AJ, West SC (2011) DNA interstrand crosslink repair and cancer. *Nat Rev Cancer* 11: 467 – 480

Dewar D, Underhill SM, Goldberg MP (2003) Oligodendrocytes and ischemic brain injury. *J Cereb Blood Flow Metab* 23: 263 – 274

Emery B (2010) Regulation of oligodendrocyte differentiation and myelination. *Science* 330: 779 – 782

French HM, Reid M, Mamontov P, Simmons RA, Grinspan JB (2009) Oxidative stress disrupts oligodendrocyte maturation. *J Neurosci Res* 87: 3076 – 3087

Friese MA, Schattling B, Fugger L (2014) Mechanisms of neurodegeneration and axonal dysfunction in multiple sclerosis. *Nat Rev Neurol* 10: 225 – 238

Gaillard H, Herrera-Moyano E, Aguilera A (2013) Transcription-associated genome instability. *Chem Rev* 113: 8638 – 8661

Girard PM, Kysela B, Harer CJ, Doherty AJ, Jeggo PA (2004) Analysis of DNA ligase IV mutations found in LIG4 syndrome patients: the impact of two linked polymorphisms. *Hum Mol Genet* 13: 2369 – 2376

Gomez-Herreros F, Schuurs-Hoeijmakers JH, McCormack M, Greally MT, Rulten S, Romero-Granados R, Counihan TJ, Chaila E, Conroy J, Ennis S, Delanty N, Cortes-Ledesma F, de Brouwer AP, Cavalleri GL, El-Khamisy SF, de Vries BB, Caldecott KW (2014) TDP2 protects transcription from abortive topoisomerase activity and is required for normal neural function. *Nat Genet* 46: 516 – 521

Hayashi S, McMahon AP (2002) Efficient recombination in diverse tissues by a tamoxifen-inducible form of Cre: a tool for temporally regulated gene activation/inactivation in the mouse. *Dev Biol* 244: 305 – 318

Herzog KH, Chong MJ, Kapsetaki M, Morgan JI, McKinnon PJ (1998) Requirement for Atm in ionizing radiation-induced cell death in the developing central nervous system. *Science* 280: 1089 – 1091

Iyama T, Wilson DM 3rd (2013) DNA repair mechanisms in dividing and non-dividing cells. *DNA Repair* 12: 620 – 636

Jana A, Pahan K (2007) Oxidative stress kills human primary oligodendrocytes via neutral sphingomyelinase: implications for multiple sclerosis. *J Neuroimmune Pharmacol* 2: 184 – 193

Jilani A, Ramotar D, Slack C, Ong C, Yang XM, Scherer SW, Lasko DD (1999) Molecular cloning of the human gene, PNKP, encoding a polynucleotide kinase 3′-phosphatase and evidence for its role in repair of DNA strand breaks caused by oxidative damage. *J Biol Chem* 274: 24176 – 24186

Karimi-Busheri F, Weinfeld M (1997) Purification and substrate specificity of polydeoxyribonucleotide kinases isolated from calf thymus and rat liver. *J Cell Biochem* 64: 258 – 272

Karimi-Busheri F, Rasouli-Nia A, Allalunis-Turner J, Weinfeld M (2007) Human polynucleotide kinase participates in repair of DNA double-strand breaks by nonhomologous end joining but not homologous recombination. *Cancer Res* 67: 6619 – 6625

Kass EM, Helgadottir HR, Chen CC, Barbera M, Wang R, Westermark UK, Ludwig T, Moynahan ME, Jasin M (2013) Double-strand break repair by homologous recombination in primary mouse somatic cells requires BRCA1 but not the ATM kinase. *Proc Natl Acad Sci USA* 110: 5564 – 5569

Katyal S, el-Khamisy SF, Russell HR, Li Y, Ju L, Caldecott KW, McKinnon PJ (2007) TDP1 facilitates chromosomal single-strand break repair in neurons and is neuroprotective in vivo. *EMBO J* 26: 4720 – 4731

Katyal S, Lee Y, Nitiss KC, Downing SM, Li Y, Shimada M, Zhao J, Russell HR, Petrini JH, Nitiss JL, McKinnon PJ (2014) Aberrant topoisomerase-1 DNA lesions are pathogenic in neurodegenerative genome instability syndromes. *Nat Neurosci* 17: 813 – 821

Kim KK, Adelstein RS, Kawamoto S (2009) Identification of neuronal nuclei (NeuN) as Fox-3, a new member of the Fox-1 gene family of splicing factors. *J Biol Chem* 284: 31052 – 31061

King IF, Yandava CN, Mabb AM, Hsiao JS, Huang HS, Pearson BL, Calabrese JM, Starmer J, Parker JS, Magnuson T, Chamberlain SJ, Philpot BD, Zylka MJ (2013) Topoisomerases facilitate transcription of long genes linked to autism. *Nature* 501: 58 – 62

Koch CA, Agyei R, Galicia S, Metalnikov P, O'Donnell P, Starostine A, Weinfeld M, Durocher D (2004) Xrcc4 physically links DNA end processing by polynucleotide kinase to DNA ligation by DNA ligase IV. *EMBO J* 23: 3874 – 3885

Lassmann H, van Horssen J, Mahad D (2012) Progressive multiple sclerosis: pathology and pathogenesis. *Nat Rev Neurol* 8: 647 – 656

Lee Y, Chong MJ, McKinnon PJ (2001) Ataxia telangiectasia mutated-dependent apoptosis after genotoxic stress in the developing nervous system is determined by cellular differentiation status. *J Neurosci* 21: 6687 – 6693

Lee Y, Katyal S, Li Y, El-Khamisy SF, Russell HR, Caldecott KW, McKinnon PJ (2009) The genesis of cerebellar interneurons and the prevention of neural DNA damage require XRCC1. *Nat Neurosci* 12: 973 – 980

Lee Y, Katyal S, Downing SM, Zhao J, Russell HR, McKinnon PJ (2012a) Neurogenesis requires TopBP1 to prevent catastrophic replicative DNA damage in early progenitors. *Nat Neurosci* 15: 819 – 826

Lee Y, Morrison BM, Li Y, Lengacher S, Farah MH, Hoffman PN, Liu Y, Tsingalia A, Jin L, Zhang PW, Pellerin L, Magistretti PJ, Rothstein JD (2012b) Oligodendroglia metabolically support axons and contribute to neurodegeneration. *Nature* 487: 443 – 448

Lee Y, Brown EJ, Chang S, McKinnon PJ (2014) Pot1a prevents telomere dysfunction and ATM-dependent neuronal loss. *J Neurosci* 34: 7836 – 7844

Madabhushi R, Pan L, Tsai LH (2014) DNA damage and its links to neurodegeneration. *Neuron* 83: 266 – 282

McKinnon PJ (2009) DNA repair deficiency and neurological disease. *Nat Rev Neurosci* 10: 100 – 112

McKinnon PJ (2013) Maintaining genome stability in the nervous system. *Nat Neurosci* 16: 1523 – 1529

Mischo HE, Gomez-Gonzalez B, Grzechnik P, Rondon AG, Wei W, Steinmetz L, Aguilera A, Proudfoot NJ (2011) Yeast Sen1 helicase protects the genome from transcription-associated instability. *Mol Cell* 41: 21 – 32

Molyneaux BJ, Arlotta P, Menezes JR, Macklis JD (2007) Neuronal subtype specification in the cerebral cortex. *Nat Rev Neurosci* 8: 427 – 437

Morrison C, Sonoda E, Takao N, Shinohara A, Yamamoto K, Takeda S (2000) The controlling role of ATM in homologous recombinational repair of DNA damage. *EMBO J* 19: 463 – 471

Nakashima M, Takano K, Osaka H, Aida N, Tsurusaki Y, Miyake N, Saitsu H, Matsumoto N (2014) Causative novel PNKP mutations and concomitant PCDH15 mutations in a patient with microcephaly with early-onset seizures and developmental delay syndrome and hearing loss. *J Hum Genet* 59: 471 – 474

O'Driscoll M, Jeggo PA (2006) The role of double-strand break repair - insights from human genetics. *Nat Rev Genet* 7: 45 – 54

Orii KE, Lee Y, Kondo N, McKinnon PJ (2006) Selective utilization of nonhomologous end-joining and homologous recombination DNA repair pathways during nervous system development. *Proc Natl Acad Sci USA* 103: 10017 – 10022

Pheiffer BH, Zimmerman SB (1982) 3′-Phosphatase activity of the DNA kinase from rat liver. *Biochem Biophys Res Commun* 109: 1297 – 1302

Poulton C, Oegema R, Heijsman D, Hoogeboom J, Schot R, Stroink H, Willemsen MA, Verheijen FW, van de Spek P, Kremer A, Mancini GM (2013) Progressive cerebellar atrophy and polyneuropathy: expanding the spectrum of PNKP mutations. *Neurogenetics* 14: 43 – 51

Rass E, Chandramouly G, Zha S, Alt FW, Xie A (2013) Ataxia telangiectasia mutated (ATM) is dispensable for endonuclease I-SceI-induced homologous recombination in mouse embryonic stem cells. *J Biol Chem* 288: 7086 – 7095

Reynolds JJ, Walker AK, Gilmore EC, Walsh CA, Caldecott KW (2012) Impact of PNKP mutations associated with microcephaly, seizures and developmental delay on enzyme activity and DNA strand break repair. *Nucleic Acids Res* 40: 6608 – 6619

Richard P, Feng S, Manley JL (2013) A SUMO-dependent interaction between Senataxin and the exosome, disrupted in the neurodegenerative disease AOA2, targets the exosome to sites of transcription-induced DNA damage. *Genes Dev* 27: 2227 – 2232

Schneider L, Fumagalli M, d'Adda di Fagagna F (2012) Terminally differentiated astrocytes lack DNA damage response signaling and are radioresistant but retain DNA repair proficiency. *Cell Death Differ* 19: 582 – 591

Segal-Raz H, Mass G, Baranes-Bachar K, Lerenthal Y, Wang SY, Chung YM, Ziv-Lehrman S, Strom CE, Helleday T, Hu MC, Chen DJ, Shiloh Y (2011) ATM-mediated phosphorylation of polynucleotide kinase/phosphatase is required for effective DNA double-strand break repair. *EMBO Rep* 12: 713 – 719

Shen J, Gilmore EC, Marshall CA, Haddadin M, Reynolds JJ, Eyaid W, Bodell A, Barry B, Gleason D, Allen K, Ganesh VS, Chang BS, Grix A, Hill RS, Topcu M, Caldecott KW, Barkovich AJ, Walsh CA (2010) Mutations in PNKP cause microcephaly, seizures and defects in DNA repair. *Nat Genet* 42: 245 – 249

Shull ER, Lee Y, Nakane H, Stracker TH, Zhao J, Russell HR, Petrini JH, McKinnon PJ (2009) Differential DNA damage signaling accounts for distinct neural apoptotic responses in ATLD and NBS. *Genes Dev* 23: 171 – 180

Stolt CC, Rehberg S, Ader M, Lommes P, Riethmacher D, Schachner M, Bartsch U, Wegner M (2002) Terminal differentiation of myelin-forming oligodendrocytes depends on the transcription factor Sox10. *Genes Dev* 16: 165 – 170

Suraweera A, Lim Y, Woods R, Birrell GW, Nasim T, Becherel OJ, Lavin MF (2009) Functional role for senataxin, defective in ataxia oculomotor apraxia type 2, in transcriptional regulation. *Hum Mol Genet* 18: 3384 – 3396

Takashima H, Boerkoel CF, John J, Saifi GM, Salih MA, Armstrong D, Mao Y, Quiocho FA, Roa BB, Nakagawa M, Stockton DW, Lupski JR (2002) Mutation of TDP1, encoding a topoisomerase I-dependent DNA damage repair enzyme, in spinocerebellar ataxia with axonal neuropathy. *Nat Genet* 32: 267 – 272

Tebbs RS, Flannery ML, Meneses JJ, Hartmann A, Tucker JD, Thompson LH, Cleaver JE, Pedersen RA (1999) Requirement for the Xrcc1 DNA base excision repair gene during early mouse development. *Dev Biol* 208: 513 – 529

Weinfeld M, Mani RS, Abdou I, Aceytuno RD, Glover JN (2011) Tidying up loose ends: the role of polynucleotide kinase/phosphatase in DNA strand break repair. *Trends Biochem Sci* 36: 262 – 271

Yeung MS, Zdunek S, Bergmann O, Bernard S, Salehpour M, Alkass K, Perl S, Tisdale J, Possnert G, Brundin L, Druid H, Frisen J (2014) Dynamics of oligodendrocyte generation and myelination in the human brain. *Cell* 159: 766 – 774

Yuce O, West SC (2013) Senataxin, defective in the neurodegenerative disorder ataxia with oculomotor apraxia 2, lies at the interface of transcription and the DNA damage response. *Mol Cell Biol* 33: 406 – 417

Zolner AE, Abdou I, Ye R, Mani RS, Fanta M, Yu Y, Douglas P, Tahbaz N, Fang S, Dobbs T, Wang C, Morrice N, Hendzel MJ, Weinfeld M, Lees-Miller SP (2011) Phosphorylation of polynucleotide kinase/phosphatase by DNA-dependent protein kinase and ataxia-telangiectasia mutated regulates its association with sites of DNA damage. *Nucleic Acids Res* 39: 9224 – 9237

 